Suppression of ferromagnetism of $CeTiGe_3$ by V substitution

W. Kittler,[1] V. Fritsch,[1] F. Weber,[2] G. Fischer,[1] D. Lamago,[2,3] G. André,[3] and H. v. Löhneysen[1,2]
[1]*Physikalisches Institut, Karlsruher Institut für Technologie, D-76131 Karlsruhe, Germany*
[2]*Institut für Festkörperphysik, Karlsruher Institut für Technologie, D-76021 Karlsruhe, Germany*
[3]*Laboratoire Léon Brillouin (CEA-CNRS), CEA-Saclay, F-91911 Gif-sur-Yvette, France*
(Received 5 August 2013; published 17 October 2013)

The crystallographic structure, magnetization, specific heat, and electrical resistivity of polycrystalline $CeTi_{1-x}V_xGe_3$ ($0 \leqslant x \leqslant 0.42$ and $x = 1$) have been studied. $CeTiGe_3$ has been reported as one of the rare ferromagnetic Kondo systems with a Curie temperature $T_c = 14$ K. We present a detailed study of the low-temperature properties on this compound, including magnetization, specific heat, and electrical resistivity in magnetic fields up to 5 T. Elastic neutron-scattering experiments confirm ferromagnetic and exclude ferrimagnetic order of $CeTiGe_3$. Analysis of the specific heat gives evidence of a strong magnetic anisotropy in this system as evidenced by a gap. Replacing Ti by V reduces T_c, with $T_c \to 0$ for $x \approx 0.35$, suggesting a possible ferromagnetic quantum critical point.

DOI: 10.1103/PhysRevB.88.165123 PACS number(s): 71.27.+a, 75.25.−j, 75.30.Kz, 75.40.−s

I. INTRODUCTION

Quantum phase transitions (QPTs) are (generally second-order) phase transitions where the critical temperature T_c is driven to $T = 0$ by a nonthermal control parameter δ such as chemical composition, pressure, or magnetic field. Here the thermal fluctuations of the magnetic transition are frozen out, so that quantum fluctuations dominate the critical behavior. As T is lowered to the quantum critical point (QCP) where $\delta = \delta_c$ and $T_c = 0$, the energy h/τ of quantum fluctuations with lifetime τ becomes larger than the thermal energy k_BT for longer and longer times τ, affecting the finite-temperature properties near a QCP as well. QPTs between different magnetic ground states have received a lot of attention in recent years. In particular, Ce and Yb systems have been investigated where the QPT arises from the competition between Ruderman-Kittel-Kasuya-Yoshida (RKKY) interaction favoring magnetic order, and the Kondo effect favoring a paramagnetic Fermi-liquid ground state.[1,2] A significant number of antiferromagnetic (AF) systems can be tuned to a QPT by hydrostatic pressure, magnetic field, or chemical substitution. Ferromagnetic (FM) QPTs, on the other hand, are quite rare among Ce and Yb systems. Recently discussed examples include $CePd_{1-x}Rh_x$ (Ref. 3) and $YbNi_4P_2$. The latter is close to a QCP but orders ferromagnetically at $T_c = 0.17$ K.[4] The theoretical description of a FM QPT is fundamentally different from the AF case, since the Hertz-Millis-Moriya (HMM) model of quantum criticality[5–7] breaks down in the FM case because here the presence of fermionic modes leads to multiple time scales.[8]

$CeTiGe_3$ is a ferromagnetic Kondo-lattice system with a Curie temperature $T_c = 14$ K. It crystallizes in the hexagonal perovskite ($BaNiO_3$-type) structure $P6_3/mmc$.[9] Here we show that magnetic order can be suppressed upon substituting Ti by V, thus making this system a possible candidate for a FM QCP. After a thorough analysis of the pure compound, we present measurements of the magnetization, electrical resistivity, and specific heat of $CeTi_{1-x}V_xGe_3$ on polycrystalline samples. Neutron powder diffraction data are used to characterize the ferromagnetic order. Our data are suggestive of a FM QCP in this compound at a V concentration $x \approx 0.35$.

II. EXPERIMENTAL DETAILS

Polycrystalline samples of $CeTi_{1-x}V_xGe_3$ were prepared from elements of high purity (Ce: 99.99%,[10] La: 99.99%,[10] Ti: 99.99%, V: 99.9%, Ge: 99.99%. Appropriate amounts were melted together in an arc-melting furnace under argon atmosphere and Ti gettering. The samples were turned over and remelted several times. After arc melting, the samples were wrapped in tantalum foil and sealed in quartz glass tubes under vacuum. The samples were then annealed for one week at 950 °C and subsequently quenched in liquid nitrogen.

X-ray powder diffraction patterns for all samples were recorded with a Siemens D500 diffractometer using the Cu K_α line. The x-ray diffraction pattern of pure $CeTiGe_3$ is presented in Fig. 1(a). The data were analyzed with the FullProf Suite software.[11]

All peaks could be clearly indexed according to the hexagonal $BaNiO_3$ structure as shown in Fig. 1(b). The inset of Fig. 1(a) reveals an impurity peak at $2\Theta = 32.07°$ (marked with an arrow) that is barely visible and could not be identified with any known binary or ternary phase of the Ce-Ti-Ge system. We estimate the amount of the impurity phase to less than 5%. X-ray data for the alloys with V substitution (not shown) were of the same quality. The lattice parameters for all $CeTi_{1-x}V_xTi_3$ samples with concentrations $0 \leqslant x \leqslant 0.42$ and $x = 1$ obtained from the corresponding diffraction pattern are shown in Fig. 2. The lattice parameters a and c nicely follow Vegard's law indicating that the Ce ions retain their valency over the whole concentration range and even up to stoichiometric $CeVGe_3$. Preliminary experiments indicate that $CeVGe_3$ orders antiferromagnetically at $T_N = 5.5$ K. Note that V substitution affects the lattice parameters to a quite different degree, with $\Delta a/a = 0.0009$ and $\Delta c/c = 0.038$ between $x = 0$ and $x = 1$. This results in a change of the c/a ratio from 0.9375 for $x = 0$ to 0.9108 for $x = 1$.

Magnetization measurements were carried out in a vibrating sample magnetometer (VSM, Oxford Instruments) and a SQUID magnetometer (MPMS, Quantum Design) in the temperature range from 1.8 K to 20 K and in external fields up to 5 T. Additionally, the magnetization $M(T)$ of $CeTiGe_3$ was measured under hydrostatic pressure of 9 kbar in a CuBe

 ©2013 American Physical Society

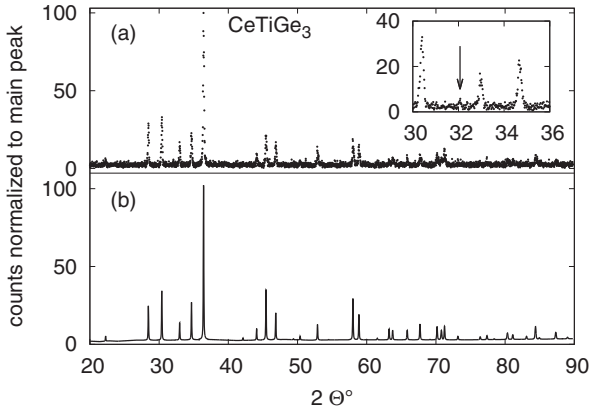

FIG. 1. X-ray pattern of $CeTiGe_3$ showing (a) experimental data and (b) the result of the Rietveld analysis using space group $P6_3/mmc$ and yielding $a = b = 6.2744$ Å, $c = 5.8823$ Å for the hexagonal structure of $CeTiGe_3$. The arrow at $2\Theta = 32.07^\circ$ in the inset of panel (a) indicates the reflection due to an unidentified impurity phase.

clamp cell in the VSM. Measurements of the field-cooled and zero-field-cooled magnetization were always performed during heating.

In order to study the magnetic structure, neutron-diffraction experiments were performed on the cold-neutron powder diffractometer G4.1 at the Laboratoire Léon Brillouin (LLB), CEA Saclay, France. We used a neutron wavelength of $\lambda = 2.4151$ Å. Data were evaluated for scattering angles $20^\circ < 2\Theta < 80^\circ$. A powder sample was obtained by crushing a polycrystal which had been previously characterized by room-temperature x-ray diffraction to have a minimal amount of impurity phase. The sample weighing 0.1 g was filled into a vanadium can and mounted in a standard ^{4}He cryostat allowing measurements between $T = 2$ K and 300 K. Neutron scattering data were analyzed using the FullProf Suite software as well.[11]

Specific-heat measurements were performed employing thermal-relaxation calorimetry in the temperature range from 1.8 to 30 K in a physical properties measurement system (PPMS, Quantum Design) equipped with an 8 T magnet. The electrical resistivity was measured in a home-built ^{4}He cryostat

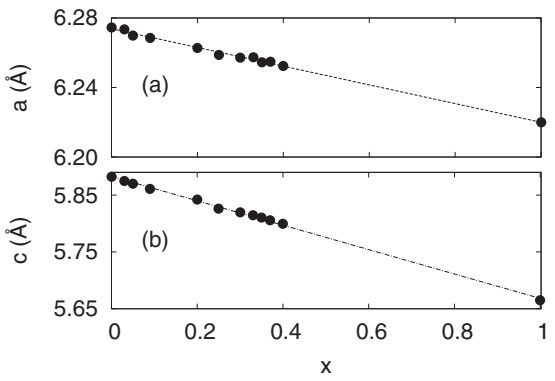

FIG. 2. Lattice parameters a (panel a) and c (panel b) of the hexagonal unit cell of $CeTi_{1-x}V_xTi_3$ for different V concentrations x. Lines are linear fits to the data. Error bars are smaller than the size of the symbols.

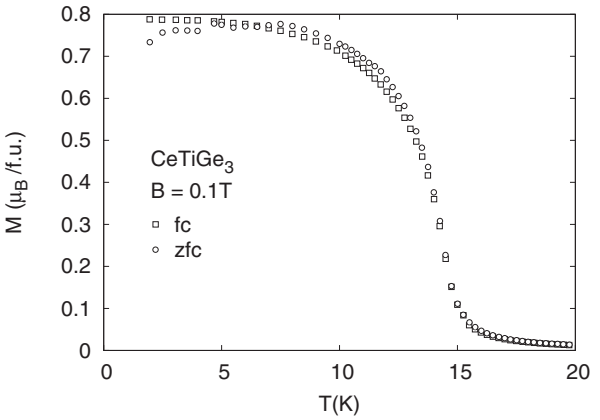

FIG. 3. Field-cooled (fc) and zero-field-cooled (zfc) magnetization M vs temperature T of a $CeTiGe_3$ polycrystal.

using a LR700 resistance bridge in 4-point contact geometry between 2.5 K and 300 K and in magnetic fields up to 5 T.

III. EXPERIMENTAL RESULTS

A. Magnetic properties of $CeTiGe_3$

Figure 3 presents the magnetization M of pure $CeTiGe_3$ vs temperature T measured in a magnetic field $B = 0.1$ T. The Curie temperature T_c is taken as the inflection point of $M(T)$, yielding $T_c = 14.3$ K in good agreement with $T_c = 14$ K reported previously.[9] The magnetization saturates at $m_s = 0.8\ \mu_B$/f.u. Only a very small difference between the field-cooled (fc) and zero-field-cooled (zfc) curve is observed indicating that the ferromagnet is almost reversible, in contrast to the work of Manfrinetti *et al.*[9] which showed a stronger fc-zfc difference. Figure 4 presents the magnetization $M(B)$ at 5 K showing a hysteresis loop, typical of ferromagnets. A closer look reveals an unusual behavior between rising and decreasing field. With rising field, the magnetization exhibits a rounded behavior before it saturates. With decreasing field the magnetization stays constant down to $B \approx 0$ and than decreases precipitously for negative field. This "asymmetric" behavior may be due to the combined effects of magnetostriction and strain in the polycrystalline sample.

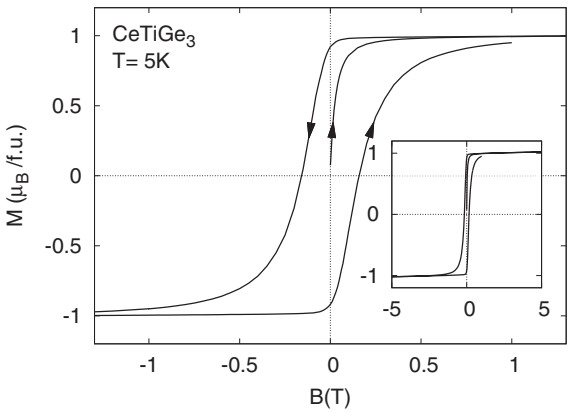

FIG. 4. Magnetization of $CeTiGe_3$ M vs magnetic field B up to 1.5 T measured at $T = 5$ K showing a hysteresis loop with the virgin zfc curve. Inset shows $M(B)$ up to 5 T.

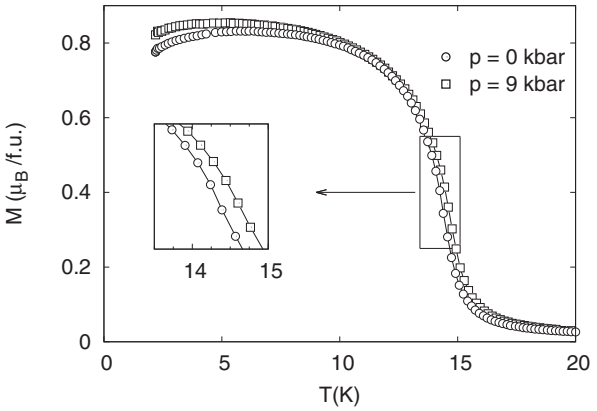

FIG. 5. Zero-field-cooled magnetization M vs temperature T of $CeTiGe_3$ measured at $B = 0.1$ T under hydrostatic pressure $p = 0$ and 9 kbar. The small difference between the data for 0 and 9 kbar is shown in the inset on an expanded T scale.

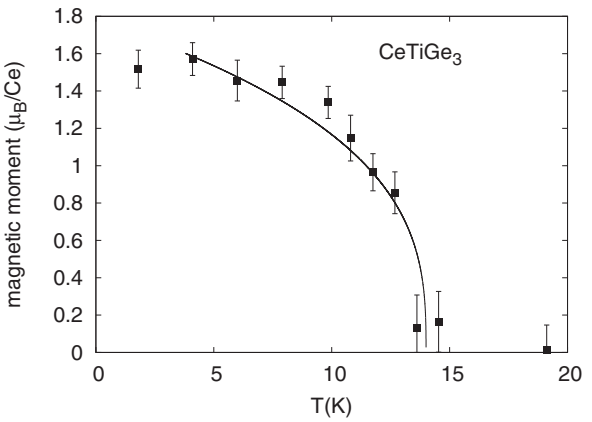

FIG. 6. Temperature dependence of the magnetic moment μ per Ce atom in $CeTiGe_3$ as obtained from neutron powder diffraction with Rietveld analysis. The line is a power-law fit of the form $(mT_c - T)^\beta$ with $\beta = 0.34$.

Figure 5 shows that the ferromagnetic order in $CeTiGe_3$ is hardly affected by hydrostatic pressure p, as can be seen from the zfc $M(T)$ curves under $p = 0$ and 9 kbar. A small increase of T_c from 14.5 to 14.8 K is observed suggesting $dT_c/dp \approx 30$ mK/kbar. This finding will be of relevance for the discussion of the effect of Ti substitution by V (see Sec. IV).

Neutron diffractograms taken in the paramagnetic phase at temperatures $T > T_c$ can be well described by a purely structural model of $CeTiGe_3$ (except for a few very small reflections that we ascribe to the impurity phase also detected by x-ray diffraction as mentioned above). We note that this parasitic contribution does not change across the ferromagnetic transition. On cooling through T_c we observe increasing diffraction intensities of several Bragg peaks. However, there is the usual complication of ferromagnets; i.e., the magnetic and lattice reflections occur at the same diffraction angles due to the identical unit cells. We found that the magnetic scattering is generally small compared to the lattice reflections. Still, at some particular scattering angles, e.g., $2\Theta = 45.8^\circ$, a relative increase of the neutron-scattering intensity of more than a factor of two on cooling through T_c can be observed. These differences in magnetic scattering intensity allow determining the direction of the ordered moments, because only the component of the magnetic moment perpendicular to the neutron scattering vector is detected.

Our neutron-scattering data at $T \leqslant 20$ K were analyzed assuming two structures in the Rietveld analysis, i.e., one for the crystallographic and one for the magnetic unit cell, with identical Bravais lattices. The resulting magnetic moment per Ce ion for $T \leqslant 15$ K is shown in Fig. 6. We note that the analysis for higher temperatures yielded zero magnetic moments within an experimental error of about ± 0.1 μ_B/Ce. Our analysis reveals that within the experimental error, the Ce moments point along the crystallographic c axis as inferred from the dependence of the magnetic scattering intensity on scattering angle. We could not detect any tilting between the Ce moments. The fitted magnetic moment per Ce atom is shown in Fig. 6. At low temperatures it reaches (1.5 ± 0.1) μ_B/Ce.

As expected, the deduced ordered magnetic moment is larger than the value of 0.8 μ_B/Ce determined from the saturated magnetization of polycrystalline $CeTiGe_3$. However, one would expect a factor-of-three difference rather than the observed factor of two. This may be attributed to texture in the polycrystalline sample leading to a preferred moment orientation while the neutron-diffraction experiment was performed with a finely mashed powder.

The temperature dependence of the ordered magnetic moment m is compatible with a power-law function of the form $m \sim (T_c - T)^\beta$ with $\beta \approx 1/3$. Since β for three-dimensional Heisenberg, XY, and Ising systems are close, we cannot make a definite statement. A much denser grid in temperature, in particular close to T_c, would be needed to determine β accurately. However, an important conclusion can be drawn from our neutron-scattering data: we do not observe any additional magnetic reflections at $T < T_c$; i.e., all additional scattering below T_c can be well described by considering only magnetic moments of Ce ions with a ferromagnetic alignment. In particular, a ferrimagnetic type of magnetic order with two different sublattice magnetizations—a possibility that was discussed in Ref. 9—can be ruled out.

B. Specific heat and electrical resistivity of $CeTiGe_3$

Figure 7 shows the specific heat $C(T)$ between 1.8 and 25 K and in zero field and in an external field $B = 1$ and 5 T. The zero-field data confirm the previous results without, however, showing an impurity contribution.[9] The sharp transition observed for $B = 0$ is completely washed out in 5 T. At At $B = 1$ T, we still observe a rather sharp maximum at a temperature that is slightly *lower* than T_c. This feature is found in reversible ferromagnets due to a rearrangement of domains to satisfy $H_i = 0$ inside the ferromagnet.[12] The entropy determined by integrating C/T vs T will be discussed in Sec. III D together with the entropy of the V-doped samples.

Figure 7(b) shows the low-T specific heat. Between 1.8 and 10 K, the data can be very well described by $C(T) = aT^{3/2}\exp(-\Delta/k_BT)$ with $\Delta/k_B = 12.9$ K. This T dependence is expected for an anisotropic ferromagnet featuring a gap in the magnetic excitation spectrum. The sizable value of $\Delta/k_B \approx 0.8T_c$ shows that the magnetic anisotropy is indeed quite strong.

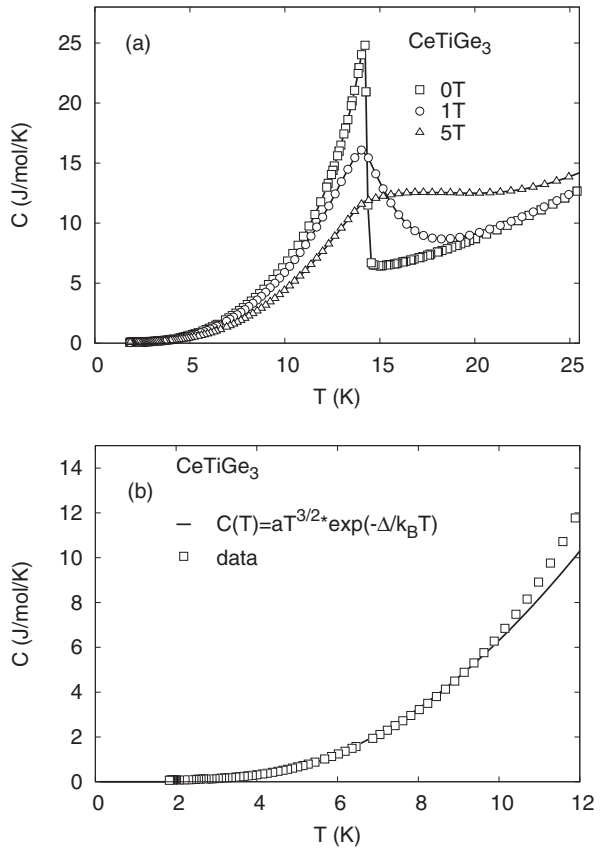

FIG. 7. Specific heat C vs temperature T of $CeTiGe_3$. (a) C vs T in fields $B = 0$, 1, and 5 T in the temperature range between 1.8 and 25 K. (b) C vs T with a fit $C(T) = aT^{3/2}\exp(-\Delta/k_BT)$.

The electrical resistivity $\rho(T)$ is depicted in Fig. 8. In the main panel of Fig. 8 the data for the low-temperature region between 2 and 30 K are shown in detail for different fields. A sharp kink at T_c is observed in zero field signaling the onset of ferromagnetism, which gives way to a rounded crossover in magnetic field. The inset shows the resistivity in zero field in the temperature range between 2 and 300 K. The resulting residual resistivity ratio RRR = 22 is an acceptable value for $CeTiGe_3$ polycrystals (RRR = 15 was reported previously for polycrystals)[9] and confirms the rather good quality of our sample. With decreasing T, $\rho(T)$ decreases to a minimum at 170 K. The rise of $\rho(T)$ towards low T is a clear indication of the Kondo effect. The maximum of ρ at 34 K marks the onset of coherence.

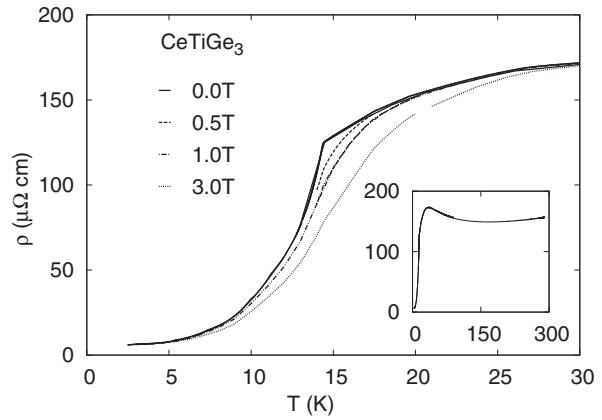

FIG. 8. Electrical resistivity ρ vs temperature T of $CeTiGe_3$ in magnetic fields $B = 0$, 0.5, 1, and 3 T.

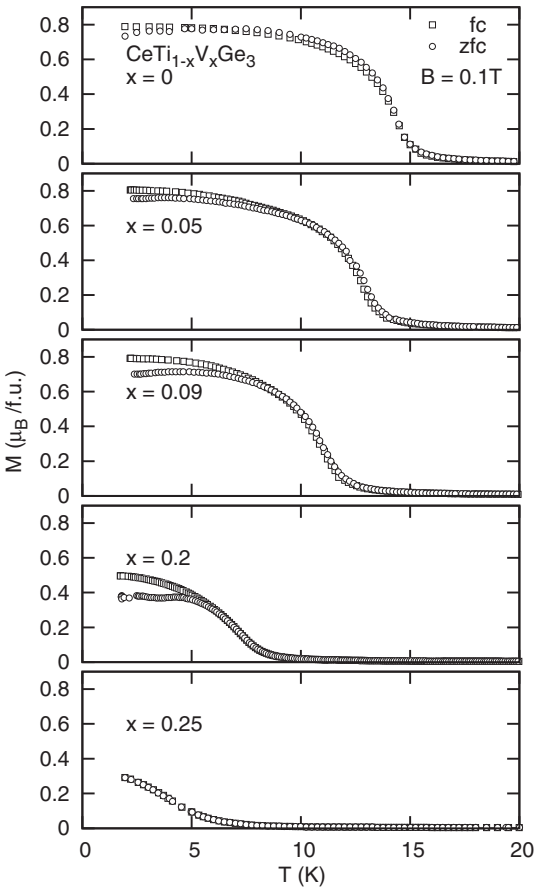

FIG. 9. fc and zfc magnetization M vs temperature T of $CeTi_{1-x}V_xGe_3$ ($x = 0$, 0.05, 0.09, 0.2, 0.25) measured in $B = 0.1$ T.

C. Magnetization and specific heat of $CeTi_{1-x}V_xGe_3$

The magnetization of $CeTiGe_3$ polycrystals with different vanadium content is shown in Fig. 9. Substituting Ti by V leads to a reduction of T_c. The ordered magnetic moment reached at low T is reduced as well. The increasing fc-zfc difference of $M(T)$ with increasing x in Fig. 9 indicates a hardening of the ferromagnetism which is expected because of the increasing disorder. The reduction of T_c with x is observed in the magnetic specific heat C_{4f} displayed in Fig. 10 as well. To obtain C_{4f}, the nonmagnetic contributions to the specific heat were estimated from a measurement of the specific heat of $LaTiGe_3$ and subtracted from the data. The ferromagnetic transition in the specific heat broadens and shifts to lower temperatures with increasing x. Figure 11 shows C_{4f}/T vs $\log T$. In this plot the broad ferromagnetic transitions for $x = 0.25$ and $x = 0.3$ can be clearly identified. The weak shoulder in C_{4f}/T at 7 K observed for $x = 0.25$ may be due to a $CeGe_2$ impurity contribution for this sample.[13] Interestingly, the C/T data above T_c for these samples exhibit an approximately logarithmic T dependence. We will come back to this point in Sec. IV.

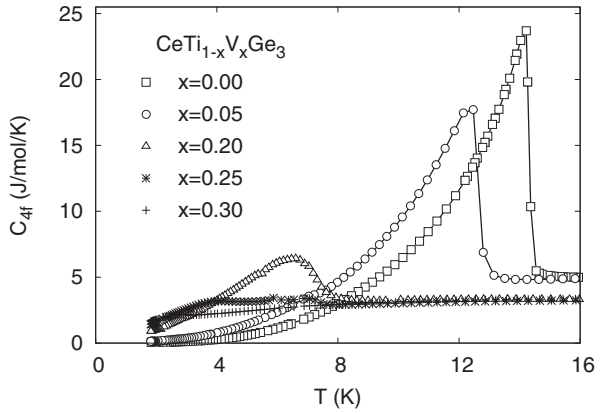

FIG. 10. $4f$-derived specific heat C_{4f} vs temperature T (C of $LaTiGe_3$ subtracted) of $CeTi_{1-x}V_xGe_3$.

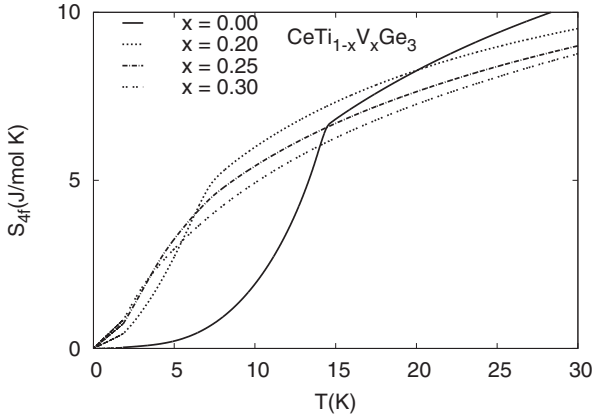

FIG. 12. $4f$-derived entropy S vs temperature T of $CeTi_{1-x}V_xGe_3$.

Figure 12 shows the $4f$-derived entropy $S_{4f}(T)$ obtained from C_{4f}. S_{4f} of all samples reach a value between 7.5 and 8.5 J/mol K at 20 K, without a systematic dependence on x. This value exeeds the value $R \ln 2 = 5.76$ J/mol K expected for a ground-state doublet considerably. A possible reason might be that the crystal-field splitting is rather small so that the entropy associated with the higher crystal-field levels comes into play. For a Ce-based heavy-fermion system with a ground-state doublet undergoing AF or FM magnetic order with $T_c < T_K$ where T_K is the effective Kondo temperature, the entropy $R \ln 2$ will be reached only at $T \gg T_K$. At $T_K \approx 35$ K corresponding to the maximum of $\rho(T)$, $S = 3.76$ J/mol K would be reached in a single-ion Kondo model.[14] This is only ≈50% of the experimentally determined entropy already acquired at 20 K. This again shows that the entropy balance requires additional low-lying excitations. Numerical calculations by Desgranges and Rasul[15] based on the Coqblin-Schrieffer model present a nice illustration of the interplay of Kondo and crystal-field (CF) effects when T_K is of the order of the CF splitting A between ground-state and first-excited-state doublets for the case $A/T_K = 2$ which might be close to the situation in $CeTiGe_3$ because in Ce intermetallics A is of the order of 60–100 K. The effect of the CF contribution to the specific heat may also be inferred from C vs T of $CeTiGe_3$, Fig. 7(a): the C_{4f} data above T_c cannot be explained by a single-ion Kondo specific heat with reasonable values of T_K under the constraint of entropy balance unless the higher CF levels are taken into account.

IV. DISCUSSION

In the remainder of this article, we will focus on a discussion of the V-substituted $CeTiGe_3$ samples. The (T,x) phase diagram of $CeTi_{1-x}V_xGe_3$ as obtained from the measurements of magnetization M, specific heat C, and electrical resistivity ρ is presented in Fig. 13. The HMM model predicts for the dependence of T_c on the control parameter tuning the QCP, in our case the V concentration x, $T_c(x) \sim |x - x_c|^{\mu}$, a critical exponent $\mu = 3/4$ and $\mu = 1$ for a FM QCP in three dimensions and two dimensions, respectively. In principle, two-dimensionality of magnetic fluctuations might arise from exchange anisotropies. Antiferromagnetic $CeCu_{6-x}Au_x$ provides an example where two-dimensional AF fluctuations arise out of three-dimensional AF order. Two-dimensional AF fluctuations lead in the HMM model to a specific-heat dependence $C/T \sim \log(T_0/T)$. Both features, a linear dependence of the Néel temperature and a logarithmic T dependence of C/T, are observed in $CeCu_{5.9}Au_{0.1}$.[16,17] Figure 13 shows that both $T_c(x)$ dependencies, $\mu = 3/4$ and $\mu = 1$, with $x_c = 0.34$ and 0.37, respectively, are compatible with the data.

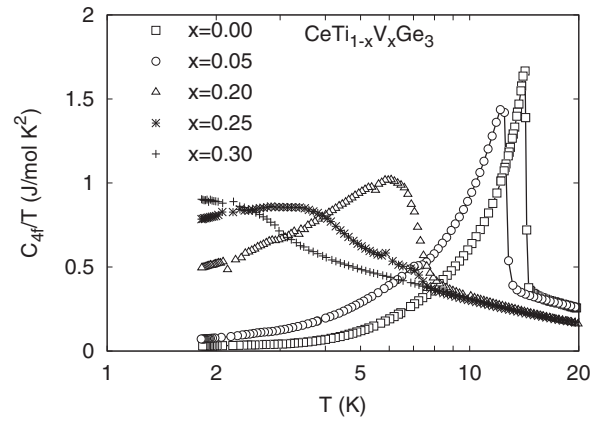

FIG. 11. $4f$-derived specific heat C_{4f} divided by T vs $\log T$ of $CeTi_{1-x}V_xGe_3$.

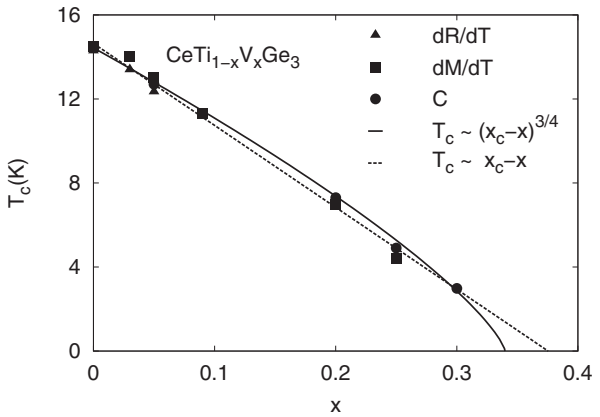

FIG. 13. T_c of $CeTi_{1-x}V_xGe_3$ for different vanadium concentrations x.

Turning to the specific heat of $CeTi_{1-x}V_xGe_3$, the data for $x = 0.3$ above $T_c = 2.8$ K vary up to 20 K as $C/T \sim \log(T_0/T)$ with $T_0 = 48$ K suggestive of three-dimensional FM fluctuations. T_0 is close to T_K as observed for heavy-fermion systems showing quantum-critical behavior. A $C/T \sim T^{-1/3}$ dependence of two-dimensional FM fluctuations is not compatible with the data. Further work will have to clarify whether a FM QCP is indeed present and, if so, whether deviations from the HMM model will be observable.

Possible deviations from the HMM model might be caused by the disorder in our V-substituted alloys. A prominent scenario is the occurrence of a quantum Griffiths phase.[18] Indeed, several reports of quantum Griffiths phases have appeared.[19,20] However, quantum tunneling of rare ordered regions within the disordered phase which leads to anomalous behavior of the thermodynamic properties[18–20] requires an isotropic spin system (Heisenberg model),[21] while $CeTiGe_3$ exhibits a strong anisotropy with a gap in the magnetic excitations as inferred above from the specific heat. Another possibility is the occurrence of a spin-glass phase near x_c. A classic example is given by the Heisenberg system $Eu_xSr_{1-x}S$ where anomalous critical exponents of the specific heat were observed upon replacement of Eu by nonmagnetic Sr.[22] Here neutron diffraction data were instrumental in distinguishing between spin-glass and inhomogeneous (reentrant) ferromagnetism.[23] This possibility will be investigated in the future on single crystals.

We have shown above that T_c of $CeTiGe_3$ increases to higher temperatures under hydrostatic pressure while substituting Ti with V does lead to a decrease of T_c. Since the unit-cell volume of $CeTi_{1-x}V_xGe_3$ decreases with x, the T_c reduction cannot be due to a volume reduction but must be attributed to a change of the electronic structure. Possibly, the increasing $3d$-electron density introduced by substituting V for Ti leads to an increase of the conduction-electron density of states at the Fermi level and hence of the Kondo coupling, thus suppressing magnetic order. Also, the strongly anisotropic change of the lattice parameters (see Sec. II) has to be taken into account. The minute pressure dependence of T_c suggests that $CeTiGe_3$ is located at the $T_c(J)$ maximum in the Doniach model,[24] where J is the exchange interaction between $4f$ electrons and conduction electrons.

V. SUMMARY

We have presented a detailed investigation of polycrystalline samples of $CeTi_{1-x}V_xGe_3$. Neutron-scattering experiments confirm the ferromagnetic nature of the magnetic order of $CeTiGe_3$ while ferrimagnetic order can be ruled out. We performed magnetization, specific-heat, and resistivity measurements to characterize the magnetic properties of pure $CeTiGe_3$. The reduction of the Curie temperature T_c upon substituting Ti by V suggests the presence of a QCP $x_c \approx 0.35$. Comparison with the positive pressure dependence dT_c/dp of pure $CeTiGe_3$ shows that the reduction of T_c upon V substitution is not due to a volume reduction, but rather has to be attributed to a change of the conduction-electron density of states. In view of the anisotropic nature of this new stoichiometric Ce system, investigation of single crystals is highly desirable and will be pursued in the future.

ACKNOWLEDGMENTS

We thank C.-L. Huang and B. Pilawa for helpful discussions and the DFG for financial support through Research Unit FOR 960 "Quantum Phase Transitions."

[1] G. Stewart, Rev. Mod. Phys. **73**, 797 (2001).
[2] H. v. Löhneysen, A. Rosch, M. Vojta, and P. Wölfle, Rev. Mod. Phys. **79**, 1015 (2007).
[3] J. G. Sereni, T. Westerkamp, R. Küchler, N. Caroca-Canales, P. Gegenwart, and C. Geibel, Phys. Rev. B **75**, 024432 (2007).
[4] C. Krellner, S. Lausberg, A. Steppke, M. Brando, L. Pedrero, H. Pfau, S. Tence, H. Rosner, F. Steglich, and C. Geibel, New J. Phys. **13**, 103014 (2011).
[5] J. A. Hertz, Phys. Rev. B **14**, 1165 (1976).
[6] A. J. Millis, Phys. Rev. B **48**, 7183 (1993).
[7] T. Moriya and T. Takimoto, J. Phys. Soc. Jpn. **64**, 960 (1995).
[8] D. Belitz, T. R. Kirkpatrick, and J. Rollbühler, Phys. Rev. Lett. **93**, 155701 (2004).
[9] P. Manfrinetti, S. Dhar, R. Kulkarni, and A. Morozkin, Solid State Commun. **135**, 444 (2005).
[10] High-purity rare-earth metals acquired from Materials Preparation Center, Ames Laboratory, US DOE Basic Energy Sciences, Ames, IA, USA, http://www.mpc.ameslab.gov
[11] J. Rodriguez-Carvajal, Physica B **192**, 55 (1993); http://www.ill.eu/sites/fullprof/.
[12] E. Scheer, H. Claus, J. Wosnitza, and H. v. Löhneysen, Phys. Rev. B **40**, 5208 (1989).
[13] H. Yashima, H. Mori, T. Satoh, and K. Kohn, Solid State Commun. **43**, 193 (1982).
[14] H.-U. Desgranges and K. Schotte, Phys. Lett. A **91**, 240 (1982).
[15] H.-U. Desgranges and J. W. Rasul, Phys. Rev. B **32**, 6100 (1985).
[16] A. Rosch, A. Schröder, O. Stockert, and H. v. Löhneysen, Phys. Rev. Lett. **79**, 159 (1997).
[17] O. Stockert, H. v. Löhneysen, A. Rosch, N. Pyka, and M. Loewenhaupt, Phys. Rev. Lett. **80**, 5627 (1998).
[18] A. H. Castro Neto, G. Castilla, and B. A. Jones, Phys. Rev. Lett. **81**, 3531 (1998).
[19] T. Westerkamp, M. Deppe, R. Küchler, M. Brando, C. Geibel, P. Gegenwart, A. P. Pikul, and F. Steglich, Phys. Rev. Lett. **102**, 206404 (2009).
[20] S. Ubaid-Kassis, T. Vojta, and A. Schroeder, Phys. Rev. Lett. **104**, 066402 (2010).
[21] T. Vojta and J. Schmalian, Phys. Rev. B **72**, 045438 (2005).
[22] J. Wosnitza and H. v. Löhneysen, Europhys. Lett. **10**, 381 (1989).
[23] H. Maletta, G. Aeppli, and S. M. Shapiro, Phys. Rev. Lett. **48**, 1490 (1982).
[24] S. Doniach, Physica B + C **91**, 231 (1977).